MOLECULAR AND CELLULAR BIOLOGY, May 1994, p. 3242–3252
0270-7306/94/$04.00+0

Vol. 14, No. 5

PEBP2αB/Mouse AML1 Consists of Multiple Isoforms That Possess Differential Transactivation Potentials

SUK-CHUL BAE,[1] EIKO OGAWA,[1] MITSUO MARUYAMA,[1] HIROYA OKA,[1] MASANOBU SATAKE,[1]†
KATSUYA SHIGESADA,[2] NANCY A. JENKINS,[3] DEBRA J. GILBERT,[3] NEAL G. COPELAND,[3]
AND YOSHIAKI ITO[1]*

Departments of Viral Oncology[1] and Genetics and Molecular Biology,[2] Institute for Virus Research, Kyoto University, Shogoin, Sakyo-ku, Kyoto 606, Japan, and Mammalian Genetics Laboratory, ABL-Basic Research Program, NCI-Frederick Cancer Research and Development Center, Frederick, Maryland 21702[3]

Received 29 November 1993/Returned for modification 3 January 1994/Accepted 14 February 1994

A murine transcription factor, PEBP2, is composed of two subunits, α and β. There are two genes in the mouse genome, *PEBP2αA* and *PEBP2αB*, which encode the α subunit. Two types of the *αB* cDNA clones, *αB1* and *αB2*, were isolated from mouse fibroblasts and characterized. They were found to represent 3.8- and 7.9-kb transcripts, respectively. The 3.8-kb RNA encodes the previously described αB protein referred to as αB1, while the 7.9-kb RNA encodes a 387-amino-acid protein, termed αB2, which is identical to αB1 except that it has an internal deletion of 64 amino acid residues. Both αB1 and αB2 associate with PEBP2β and form a heterodimer. The αB2/β complex binds to the PEBP2 binding site two- to threefold more strongly than the αB1/β complex does. αB1 stimulates transcription through the PEBP2 site about 40-fold, while αB2 is only about 25 to 45% as active as αB1. Transactivation domain is located downstream of the 128-amino-acid *runt* homology region, referred to as the Runt domain. Mouse chromosome mapping studies revealed that *αA*, *αB*, and β genes are mapped to chromosomes 17, 16, and 8, respectively. The last two genes are syntenic with the human *AML1* on chromosome 21q22 and *PEBP2β/CBFβ* on 16q22 detected at the breakpoints of characteristic chromosome translocations of the two different subtypes of acute myeloid leukemia. These results suggest that the previously described chimeric gene products, AML1/MTG8(ETO) and AML1-EAP generated by t(8;21) and t(3;21), respectively, lack the transactivation domain of AML1.

A murine transcription factor, PEBP2, also called PEA2, was identified as a factor which binds to the region of the polyomavirus enhancer originally termed the PEA2 site (35). PEBP2 functionally cooperates with other enhancer core-binding proteins, including AP1 and Ets family proteins, PEA3 (48), PEA3-91 (20), and PEBP5 (2), and plays an important role in stimulation of transcription and viral DNA replication. PEBP2 is composed of α and β subunits (32, 34). The α subunit bind to DNA by recognizing the consensus sequence, (Pu/T) ACCPuCA (13, 34). The companion β subunit binds to the α protein and increases the affinity of the α protein to DNA without binding to DNA by itself (32). cDNAs coding for both subunits have been cloned and characterized in detail (32, 34).

PEBP2 has recently been shown to be closely related to acute myeloid leukemia (AML). The t(8;21)(q22;q22) translocation is one of the most frequent chromosome abnormalities in AML and is classified into the FAB-M2 subtype of AML (39). It has been shown that the t(8;21) breakpoints in the chromosome 21 are clustered in the recently described *AML1* gene (27), the product of which shares a high homology within the 128-amino-acid (aa) region with the product of the *Drosophila* segmentation gene, *runt* (14), and the α subunit of PEBP2 (8, 9, 34). The evolutionarily conserved region of the PEBP2α protein contains both the DNA binding and heterodimerizing activities. It has been proposed that this conserved region be named the Runt domain (12). cDNA cloning revealed that there is at least one additional gene in the mouse genome, *αB*, which shares a high sequence homology with the original α gene, termed *αA*. The *αB* gene as a whole is highly homologous to human *AML1* (3). The discovery of the homology of the AML1 protein to the αsubunit of PEBP2 suggested that the AML1 protein may act as a transcription factor. However, this has not been directly demonstrated.

The C-terminal end of the evolutionarily conserved *runt* homology region is defined by an exon-intron junction in the AML1 protein (27), and the t(8;21) breakpoints consistently occur within this intron (9, 15, 22, 26, 27, 30, 42, 46). As a result, the t(8;21) translocations juxtapose the 5′ portion of the *AML1* gene with the *MTG8(ETO)* gene on chromosome 8, resulting in the synthesis of an *AML1/MTG8(ETO)* fusion transcript (9, 15, 26, 27, 29, 30). The importance of the role of AML1/MTG8(ETO) fusion protein in the pathogenesis of this type of leukemia has been suggested (40). *AML1* is also found at the breakpoints of t(3;21)(q26;q22) translocation in therapy-related leukemia and in chronic myeloid leukemia in blast crisis. The breakpoints of t(3;21) are clustered within a different intron located further downstream of the breakpoint cluster region of t(8;21). As a result of this translocation, the *AML1-EAP* fusion transcript is synthesized (31).

Like *Drosophila* Runt protein, PEBP2 appears to be involved in transcriptional regulation in multiple pathways. One of the roles of PEBP2 is its involvement in T-cell-specific gene expression (16, 34, 37). Recent cDNA cloning revealed that the murine factor termed CBF is identical to PEBP2 (47). Judging from the recognition sequences and other properties, PEBP2/CBF is probably identical or related to factors variously referred to as SEF-1 (45), S/A-CBF (4), NF-dE3A (37), and MyNF1 (44).

To add to the complexity of PEBP2-mediated gene regulation, each subfamily of PEBP2α has been found to produce

* Corresponding author. Phone: 81-75-751-4028. Fax: 81-75-752-3232. Electronic mail address: yito@virus.kyoto-u.ac.jp.

† Present address: Department of Molecular Immunology, Institute of Development, Aging and Cancer, Tohoku University, 4-1, Aoba-ku, Sendai 980, Japan.

multiple transcripts of various sizes in a cell-type-dependent manner (3, 34). Northern (RNA) blot analyses showed that the mouse *AML1/αB* gene, referred to hereafter as *PEBP2αB*, generates mRNAs of four major size classes (7.9, 6.2, 3.8 to 4.2, and 2.1 kb) in cultured hematopoietic cell lines (3). A very similar expression pattern of human *AML1* was observed in leukemic cell lines of human myeloid lineage and normal bone marrow cells (26, 40). Northern blotting with higher resolution revealed that each of the major size class RNAs is composed of multiple subspecies. Of these, only the 7.9- and 3.8-kb species were detected in Ha-*ras*-transformed NIH 3T3 cells (3). Thus, the question emerges as to what specific regulatory roles these mRNA subspecies have and how their differential synthesis is controlled.

As the first step to characterize the transcripts and their products of *PEBP2αB*, we decided to examine two mRNA species from mouse fibroblasts and their products. The cDNA sequences revealed that the 3.8-kb species encodes the αB1 protein reported previously (3). The 7.9-kb species, on the other hand, encodes the protein identical to the αB1 protein except for an internal deletion of 64 aa located immediately downstream of the Runt domain. Comparison of these two cDNA clones and their protein products revealed some basic features of the transcriptional control mechanism employed by *AML1*. Some insights into the functions of the AML1/MTG8 (ETO) and AML1-EAP chimeric proteins are also provided by these results.

MATERIALS AND METHODS

Chromosomal mapping of *Pebpa2a*, *Pebpa2b*, and *Pebpb2* in the mouse genome. The genes were mapped by interspecific backcross analysis. References for the map positions of most human loci can be obtained from GDB (Genome Data Base), a computerized data base of human linkage information maintained by The William H. Welch Medical Library of The Johns Hopkins University (Baltimore, Md.).

Interspecific backcross progeny were generated by mating (C57BL/6J × *Mus spretus*)F_1 females and C57BL/6J males as described previously (7). A total of 205 N_2 mice were used to map three loci: *PEBP2αA* (*Pebpa2a*), *PEBP2αB* (*Pebpa2b*), and *PEBP2β* (*Pebpb2*). All blots were prepared with Zetabind nylon membranes (AMF-Cuno). Probes were labeled with [α-^{32}P]dCTP, using a random priming labeling kit (Amersham) or a nick translation labeling kit (Boehringer Mannheim). The *Pebpa2a* probe, a 1,997-bp *Kpn*I fragment of mouse cDNA (34), detected fragments of 6.8 kb in C57BL/6J (B) DNA and 3.2 kb in *M. spretus* (S) DNA following digestion with *Hin*dIII. The *Pebpa2b* probe containing nucleotides (nt) 1 through 1788 of the αB1 cDNA (3) detected *Bgl*II fragments of 18.0, 7.6, 6.0, and 2.5 kb (B) and 18.0, 10.0, 7.6, and 2.5 kb (S). The *Pebpb2* probe, containing nt 171 through 2297 of the β2 cDNA (32), detected major *Sph*I fragments of 5.4 (B) and 4.5 (S) kb. The presence or absence of *M. spretus*-specific fragments was monitored in backcross mice.

Descriptions of the probes and restriction fragment length polymorphisms (RFLPs) for several of the loci used to position these genes in the interspecific backcross has been reported; these include *H-2*, *Mep-1a*, *Vav*, and *Fer* on chromosome 17 (11) and *Ets-2* on chromosome 16 (43). Several loci have not been reported previously for our interspecific backcross. The probe for amyloid beta (A4) precursor protein (*App*) was a 1.0-kb *Eco*RI fragment of mouse cDNA that detected major *Sca*I fragments of 2.8 (B) and 5.0 (S) kb. The presence or absence of the *M. spretus* fragment was monitored in backcross mice. The probe for myxovirus resistance 1 (*Mx-1*) was a 2.3-kb *Bam*HI fragment of mouse cDNA that detected *Hin*cII fragments of 7.4, 4.8, 3.4, 3.0, 2.3, 1.5, 1.3, and 0.3 kb (B) and 8.0, 5.8, 3.4, 3.0, 2.3, 2.1, 1.5, 1.3, and 0.3 kb (S). The 8.0-, 5.8-, and 2.1-kb *Hin*cII *M. spretus*-specific RFLPs cosegregated and were monitored in this analysis. Finally, the probe for the c-*maf* proto-oncogene (*Maf*) was a 750-bp *Xba*I fragment of avian proviral v-*maf* DNA that detected major *Sac*I fragments of 9.0 and 3.4 kb (B) and 4.0 and 3.4 kb (S). The inheritance of the 4.0-kb *Sac*I RFLP was monitored. Recombination distances were calculated by using the computer program SPRETUS MADNESS. Gene order was determined by minimizing the number of recombination events required to explain the allele distribution patterns.

cDNA library and its screening. A cDNA library constructed from cytoplasmic polyadenylated RNA of Ha-*ras*-transformed NIH 3T3 cells by using plasmid vector pSI4001 (34) was screened by the colony hybridization method (19). Colonies (1.2×10^6) were screened at a density of 10^4 colonies per filter (82-mm diameter). The 1.7-kb *Eco*RI restriction fragment of *PEBP2αB1* cDNA was labeled by the multiprimer DNA labeling method (Amersham) and used as a probe (3).

Screening and characterization of genomic clones. An EMBL3 mouse genomic DNA library prepared from the *Sau*3AI partially digested DNA from a strain 129 mouse was screened by the plaque hybridization method (19). The 1.7-kb *Eco*RI fragment of *αB1* cDNA was used as a probe. Among the positive clones, the clone containing the 3′ end of αB2 cDNA was selected by PCR, using the sense primer 5′-CCTGTGCAGGATGCTCCTCA (nt 4041 to 4060) and the antisense primer 5′-GAGCACATGTATGTCAGAAC (nt 4269 to 4288). Phage DNA obtained from clone αBG-55 resulted in generation of a PCR product of the expected size of 248 bp. αBG-55 contains about 15 kb of genomic DNA. Restriction enzyme sites of the clone were mapped, and the DNA fragments containing exons were subcloned into Bluescript phagemid. The nucleotide sequence was analyzed by dideoxy DNA sequencing.

Sequencing and computer analysis. DNA sequencing was performed on double-stranded templates, using internal oligonucleotide primers or flanking vector primers, by standard protocols (Exo/Mung deletion kit [Stratagene] and Sequenase DNA sequencing kit [United States Biochemical Corporation]). Any ambiguities were resolved by using dITP instead of dGTP. The positions where *PEBP2αB2* differed from *PEBP2αB1* were checked in several independent clones. To search for homologous amino acid sequences, the GenBank and EMBL data bases were screened by the BLAST program (1).

Northern blot analysis of *PEBP2αB2* mRNA. RNA from Ha-*ras*-transformed NIH 3T3 cells was prepared by the acid-guanidinium thiocyanate-phenol chloroform extraction method (6). Poly(A)$^+$ RNA was selected by oligo(dT)-cellulose column chromatography. Five micrograms of poly(A)$^+$ RNA was separated on a 1.2% agarose–formaldehyde gel and transferred to a nylon membrane (Zeta-probe; Bio-Rad). The blot was hybridized with ^{32}P-labeled probes composed of the *Bst*EII-*Sma*I (probe A; Fig. 1) or the *Eco*RV-*Sph*I (probe B; Fig. 1) fragment of *PEBP2αB2* cDNA or the ΔαB2 region of the *αB1* cDNA prepared by PCR amplification (probe C; Fig. 1). Prehybridization, hybridization to multiprimer-labeled probes, and washing were performed as instructed by the manufacturer (Bio-Rad).

Construction of deletion mutants. The two deletion mutants, αB1(1–243) and αB1(1–185), which contain the coding regions of the corresponding number of amino acids, were constructed by recombinant PCR (25). For the construction of

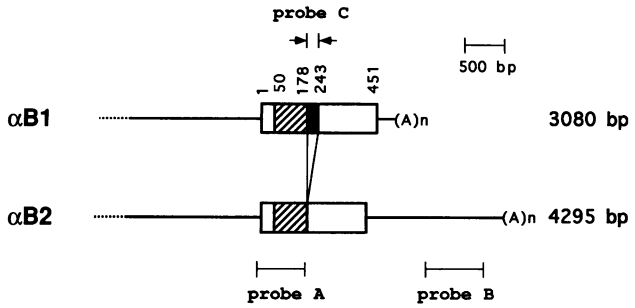

FIG. 1. Schematic diagram of the *PEBP2αB1* and *PEBP2αB2* cDNAs. The longest cDNA clones of the *αB1* and the *αB2* cDNAs are represented by horizontal thick bars for untranslated regions and by boxes for open reading frames deduced from the nucleotide sequences. The entire *αB1* cDNA sequences overlaps with the *αB2* cDNA sequences except for the poly(A) track and the alternatively spliced exon, ΔαB2 (see text). The Runt domain (hatched box) and ΔαB2 (gray box) are indicated. Nucleotide numbers on the right represent the lengths of the cDNAs except for poly(A) sequences. Numbers over the boxes represent amino acid numbers of αB1 (3). Dotted lines, representing the regions remaining to be cloned, are not to scale. The regions of the cDNA used as probes A, B, and C for Northern blot analyses are indicated.

αB1(1–185), two PCRs were performed separately with (i) primers PA (5′-TGAGGAGCGGCGACCGCAGCATGGT, sense, nt 1704 to 1728) and PB (5′-AGCTCAGTAGGCTA GTTTCTGCCGATGTC, antisense recombinant primer) and (ii) primer PC (5′-CGGCAGAAACTAGCCTACTGAGCT GAGCG, sense recombinant primer) and the SK sequencing primer (Stratagene), using plasmid pKS-αB1 as a template. pKS-αB1 contains 1.7 kb of *PEBP2αB1* cDNA in the *Eco*RI site of the KS Bluescript II vector (3). The two PCR products were separated on a 1.5% agarose gel and recovered from the gel. After the primary PCR products were mixed together, secondary PCR was performed for 12 cycles in the absence of primers. Reaction conditions were 50 s at 94°C, 1 min at 50°C, and 2 min at 72°C. The recombinant PCR product was digested with restriction enzyme *Bst*EII located in the Runt domain coding region and *Xba*I located in the flanking vector sequence. The double-digested PCR product was ligated into *Bst*EII-*Xba*I double-digested pKS-αB1. αB1(1–243) was constructed by the same way except for the primers used for primary PCR. In the case of the αB1(1–243) deletion construct, primer pairs PA- and PD (5′-CGCTCAGCTCAGTAG GCCTGCATCTGACTTTG, antisense recombinant primer) and PE (5′-CAAAGTCAGATGCAGGCCTA CTGAGCT GAGCG, sense recombinant primer)-SK were used for primary PCR. DNA sequences of the constructed mutants were verified by dideoxy DNA sequencing.

In vitro translation. PEBP2αB1, PEBP2αB2, and deletion mutants were subcloned into Bluescript II phagemid (Stratagene). Capped RNA was synthesized from linearized vector with T3 or T7 RNA polymerase as instructed by the manufacturer (mRNA capping kit; Stratagene). RNA was quantitated by UV absorption, and its integrity was verified by gel electrophoresis. An optimized amount of RNA was used to synthesize each protein in rabbit reticulocyte lysate (Promega). The efficiency of synthesis of full-length protein was checked by both incorporation of radioactive precursors ([^{3}H]leucine) and sodium dodecyl sulfate-polyacrylamide gel electrophoresis (SDS-PAGE) followed by fluorography and densitometric analysis.

DNA binding assay. A PEBP2 site containing double-stranded DNA probe ΔF9-5000 (5′-AACTGACCGCAGCTG GCCGTGCGA) was prepared and used for electrophoresis mobility shift assays (EMSA) as described previously (13). All binding assays were performed at 30°C for 30 min in 20 μl of 20 mM *N*-2-hydroxyethylpiperazine-*N*′-2-ethanesulfonic acid (HEPES; pH 7.6)–4% (wt/vol) Ficoll type 400–2 mM EDTA–2 μg of poly(dI-dC), using 0.05 to 1 nM ^{32}P-end-labeled probe with T4 kinase. The competition assay was done in the presence or absence of the unlabeled synthetic 17-bp duplex containing SL3-3 enhancer core sequences (5′-GTGCTTAAC CACAGATA [13, 45]). PEBP2 binding sites are underlined. Half of each reaction mixture was loaded on a 0.25× Tris-borate-EDTA–5% nondenaturing polyacrylamide gel, electrophoresed at 250 V for 1 h, and autoradiographed for 16 h at −70°C.

Transfection experiments and CAT assay. Reporter plasmids pTβ3W4W-tkCAT and pTβ3M4M-tkCAT, which contain the T-cell receptor (TCR) β enhancer fragment harboring two PEBP2 sites (Tβ3 and Tβ4; nt 620 to 735 of the TCR β enhancer [16]) and its mutated version of PEBP2 sites, respectively, were constructed from pBL2CAT (18) as described previously (34). pTβ3M4M-tkCAT contains mutations in both PEBP2 sites (Tβ3, TGTGGTT-TGTCGTG at nt 627 to 632; Tβ4, AACCACA-CACGACA at nt 708 to 714). Effector plasmids pEF-αA1, -αB1, -αB2, -αB(1–243), and -αB(1–185) were constructed so as to contain the whole coding region of αA1, αB1, and αB2 and the deletion versions of αB1 at the *Xba*I site of pEF-BOS from which the simian virus 40 replication origin region was deleted (28). P19 cells were transfected as described by Chen and Okayama (5), and cell extracts were prepared 48 h after transfection. Chloramphenicol acetyltransferase (CAT) activities were determined by the standard protocol (41).

Nucleotide sequence accession numbers. The nucleotide and predicted amino acid sequence data reported in Fig. 3 appear in the GSDB, DDBJ, EMBL, and NCBI data bases under accession number D26532. The sequence shown in Fig. 4 has been assigned DDBJ accession number D26531.

RESULTS

Chromosome mapping of *PEBP2αA*, *-αB* and *-β* genes. The murine chromosomal locations of three genes, *Pebpa2a*, *Pebpa2b*, and *Pebpb2*, encoding PEBP2αA, PEBP2αB, and PEBP2β, respectively, were determined by using an interspecific backcross mapping panel derived from [(C57BL/6J × *M. spretus*)F_1 × C57BL/6J] mice. cDNAs representing each of the loci were used as probes in Southern blot hybridization analysis of C57BL/6J and *M. spretus* genomic DNA that was separately digested with several different restriction enzymes to identify informative RFLPs useful for gene mapping (see Materials and Methods). The strain distribution pattern of each RFLP in the interspecific backcross was then determined by monitoring the presence or absence of RFLPs specific for *M. spretus* in backcross mice. Each of these genes mapped to a single chromosome location. The mapping results (Fig. 2) assigned the three loci to three different mouse autosomes, indicating that the three genes have become well dispersed throughout evolution.

Pebpa2a mapped to the central region of mouse chromosome 17, 8.7 centimorgans (cM) distal of *H-2* and 9.5 cM proximal to *Vav*. *Pebpa2b* mapped to the distal region of mouse chromosome 16, 2.3 cM distal of *App* and 2.3 cM proximal to *Ets-2*. *Pebpb2* mapped to the distal region of mouse chromosome 8, 7.2 cM distal of *Mt-1* and 0.9 cM proximal to *Hp*.

The distal region of mouse chromosome 16 shares a region

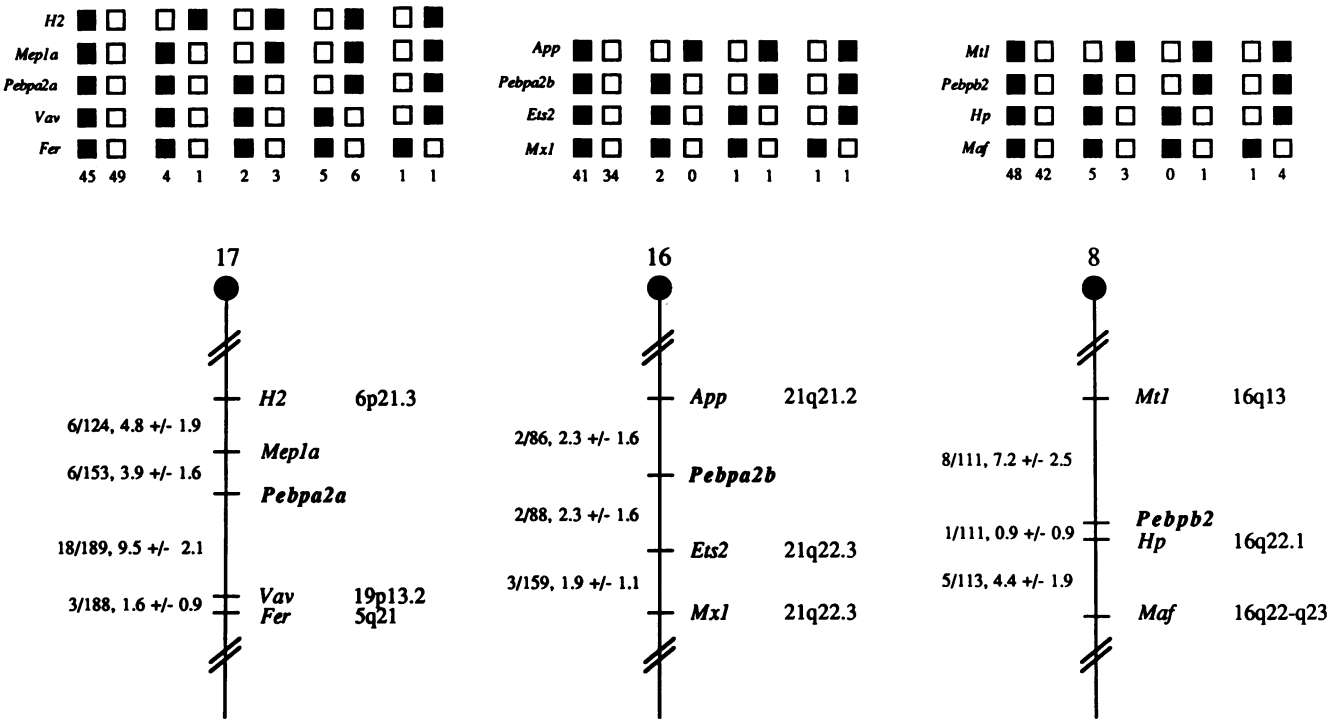

FIG. 2. Chromosomal locations of *Pebpa2a*, *Pebpa2b*, and *Pebpb2* in the mouse genome. *Pebpa2a*, *Pebpa2b*, and *Pebpb2*, encoding PEBP2αA, PEBP2αB, and PEBP2β, respectively, were mapped by interspecific backcross analysis. The segregation patterns of these loci and flanking genes in backcross animals that were typed for all loci are shown above the chromosome maps. For individual pairs of loci, more animals were typed (see below). Each column represents the chromosome identified in the backcross progeny that was inherited from the (C57BL/6J × *M. spretus*)F_1 parent. Shaded boxes represent the presence of a C57BL/6J allele, and white boxes represent the presence of an *M. spretus* allele. The number of offspring inheriting each type of chromosome is given below each column. Partial chromosome linkage maps showing the location of the *Pebp* loci in relation to linked genes are also shown. The number of recombinant N_2 animals is presented over the total number of N_2 animals typed to the left of the chromosome maps between each pair of loci. The recombination frequencies, expressed as genetic distance in centimorgans (±1 standard error), are also shown. Gene order was determined by minimizing the number of recombination events required to explain the allele distribution patterns. The positions of loci on human chromosomes, where known, are shown to the right of the chromosome maps.

of homology with human chromosome 21q21-q22 (summarized in Fig. 2). Thus, we would expect the human homolog of *Pebpa2b* to be located on 21q21-q22 as well. It has recently been shown that *AML1* maps to 21q22 (27). These linkage studies further support the notion that *Pebpa2b* is the authentic mouse homolog of *AML1*. Similarly, *Pebpb2* maps in a region of mouse chromosome 8 that is homologous with human 16q (Fig. 2). The sequence comparison revealed that the gene on 16q22 indeed encodes the human homolog of PEBP2β/CBFβ (17). The human homolog of *Pebpa2a* has not yet been mapped. However, on the basis of mouse-human linkage homologies, we suspect that the gene resides on human 6p, 19p, or 5q (Fig. 2).

Identification of two isoforms of *PEBP2αB* cDNAs. Nine cDNA clones isolated from the cDNA library prepared from Ha-*ras*-transformed NIH 3T3 cells were classified into two types consisting of four and five clones each. The longest cDNAs of each type were 3.1 and 4.3 kb, respectively, and their nucleotide sequences were determined. A diagrammatic representation of the two types of cDNAs is shown in Fig. 1. The sequence analysis revealed that the predicted protein product of the shorter cDNA was identical to the αB protein, to be referred to as αB1, that we described earlier (3). On the other hand, the predicted product of the longer cDNA was identical to αB1 except that there was a 64-aa-long internal deletion (to be referred to as ΔαB2) and one amino acid substitution, from arginine to asparagine, at the junction of the deletion. We will refer to these cDNAs as *PEBP2αB1* and *PEBP2αB2* cDNAs, respectively. The protein encoded by *PEBP2αB2* will be referred to as αB2. The entire nucleotide sequence of the 4.3-kb-long *PEBP2αB2* cDNA is shown in Fig. 3.

The 3.1-kb-long *αB1* cDNA has a 160-base-long 3′ noncoding region and a 1.6-kb-long 5′ noncoding region. All sequences of the *αB1* cDNA are included in the 4.3-kb cDNA except for the poly(A) tail and the 192-bp ΔαB2 segment within the coding region. There is a poly(A) addition signal 27 bp upstream of the poly(A) sequence. As will be shown below, this cDNA species represents 3.8-kb RNA. Therefore, the 5′-terminal message spanning approximately 0.7 kb must be still missing from this cDNA. As will also be shown below, the 4.3-kb αB2 cDNA represents a 7.9-kb RNA species. The *αB2* cDNA extends toward the 3′ direction by 1,400 bp beyond the poly(A) addition site used by the *αB1* cDNA. Even though polyadenylation has clearly occurred, there is no typical poly(A) addition signal (AATAAA), or a variant with less than two mismatches, in the vicinity of the poly(A) stretch at the 3′ end of the 4.3-kb cDNA. To examine whether this apparent lack of a polyadenylation signal is due to an artifact of cloning, we isolated and sequenced the mouse genomic clone corresponding to this region. The result revealed that the cDNA and the genomic sequences are identical up to the last nucleotide before the poly(A) stretch (Fig. 4). The genomic DNA did not have any A-rich stretch at this site. Therefore, the poly(A) stretch of the 4.3-kb cDNA represents the genuine poly(A)

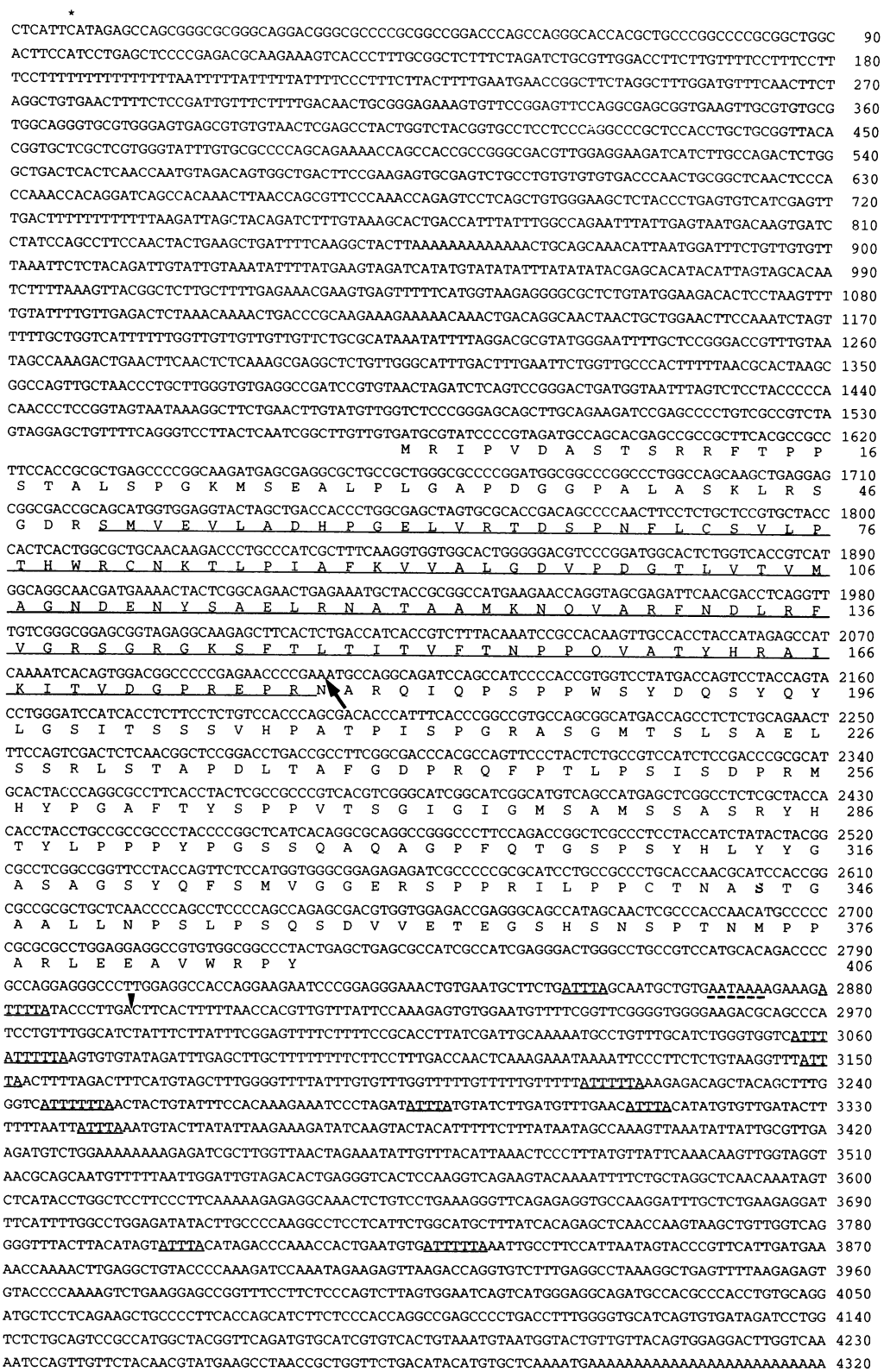

FIG. 3. Nucleotide sequence of the *PEBP2αB2* cDNA. The nucleotide sequence of the longest cDNA of *PEBP2αB2* is shown above the sequence of predicted protein product. The longest *αB1* cDNA has a 5′ untranslated sequence only six bases shorter than that of the *αB2* cDNA. The start site of the *αB1* cDNA is indicated by an asterisk. The Runt domain is underlined. The arrow indicates where the sequence encoding the ΔαB2 region is inserted in the *αB1* cDNA. It also corresponds to the t(8;21) translocation breakpoints in human *AML1*. The polyadenylation site and signal sequence (AATAAA) of the *αB1* cDNA are marked by an arrowhead and a dotted line, respectively. Putative mRNA-destabilizing sequences are underlined.

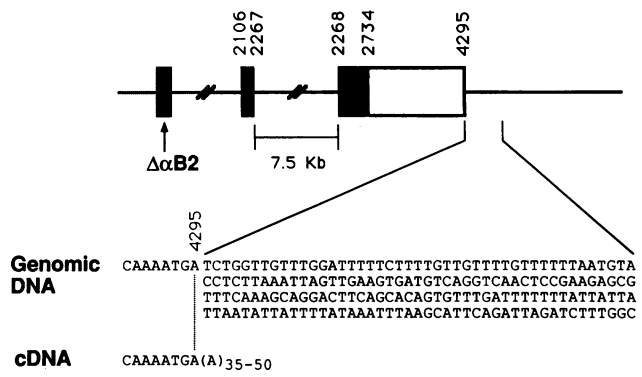

FIG. 4. Genomic DNA structure surrounding the polyadenylation site of the *PEBP2αB2* gene transcript. Exons are shown as boxes. Coding and noncoding regions are indicated by black and white boxes, respectively. ΔαB2 (gray box) is shown to be an exon in the human *AML1* genomic organization (27). Nucleotide numbers of the *αB2* cDNA are given above the diagram. The nucleotide sequences of the *αB2* cDNA and the genomic DNA surrounding the polyadenylation site are shown.

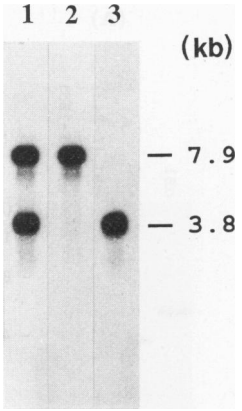

FIG. 5. The *αB1* and *αB2* cDNAs represent 3.8- and 7.9-kb mRNAs, respectively. Five micrograms of poly(A)$^+$ RNA from Ha-*ras*-transformed NIH 3T3 cells was electrophoresed in each of the three lanes and analyzed by Northern blotting with the three *αB* cDNA probes shown in Fig. 1 (lane 1, probe A; lane 2, probe B; lane 3, probe C).

tail. Poly(A) tails not preceded by a typical AAUAAA motif have been described for alternatively polyadenylated c-*abl* (23) and cyclin D (49) mRNAs. These results further suggest that the 4.3-kb cDNA lacks about 3.6 kb from the 5′ untranslated region of the 7.9-kb RNA. The *AML1/MTG8* cDNA clones representing the 6.2- and 7.8-kb fusion transcripts contain *MTG8* sequences with poly(A) stretches spanning less than 2 kb (15, 26). The results also suggest the presence of *AML1* mRNA species with an extremely long 5′ noncoding region. Recently, however, we isolated from a mouse T-cell library a cDNA clone which contains a 3′ noncoding region longer than that of the *αB2* cDNA (unpublished data). Determination of the precise structure of these RNAs, therefore, must await isolation of full-length cDNAs. It is worth noting that there are 12 copies of the $AT_{3-6}A$ motif known as an mRNA-destabilizing signal in the 3′ noncoding region. Ten are clustered within the first 600 nt, counting from the end of the coding region. Eight of them are present only in the *αB2* cDNA.

Each RNA species encodes a distinct isoform of the αB protein. The preceding analysis of cDNA clones suggested that αB1 and αB2 are encoded in 3.8- 7.9-kb RNAs, respectively. Further evidence supporting this assignment was obtained from the following Northern blot analysis.

When the RNA extracted from Ha-*ras*-transformed NIH 3T3 cells was probed with region A of the *αB* cDNA shown in Fig. 1 encoding the Runt domain, both the 7.9- and 3.8-kb-long species were clearly detected (Fig. 5, lane 1) as described previously (3). When probe B (Fig. 1) unique to the 4.3-kb *αB2* cDNA was used, only the 7.9-kb species was detected (lane 2). On the other hand, the probe C (Fig. 1) unique to the 3.1-kb *αB1* cDNA hybridized exclusively with the 3.8-kb RNA (lane 3).

The results shown in Fig. 5 could not rule out the possibility that the 3.8-kb RNA encodes both αB1 and αB2. However, all of the five cDNA clones belonging to the 3.1-kb cDNA class that we isolated encoded the αB1. Therefore, the majority, if not all, of the 3.8-kb RNA is likely to encode αB1. This, in turn, raises an intriguing possibility that the splicing event to eliminate the ΔαB2 exon is specifically coupled to the selective use of the distal polyadenylation site and probably also to the generation of the longer 5′ untranslated region predicted for 7.9-kb RNA, at least in Ha-*ras*-transformed NIH 3T3 cells.

αB1 and αB2 bind to DNA and associate with β2. Figure 6 diagrammatically shows the structures of αB1 and αB2 with the nucleotide and amino acid sequences of ΔαB2. Figure 6 also illustrates the predicted products of two artificial deletion constructs, αB1(1–243) and αB1(1–185). The αB1(1–243) is very similar to the previously described 250-aa protein encoded by human *AML1*: first 241-aa sequences of the two proteins are identical except for three conserved amino acid substitutions. The encoded proteins were in vitro translated and analyzed by SDS-PAGE (Fig. 7A). These proteins were subjected to EMSA. As shown in Fig. 7B, the αB1, αB2, αB1(1–243), and αB1(1–185) proteins all bound to the PEBP2 site (lanes 1, 4, 7, and 10).

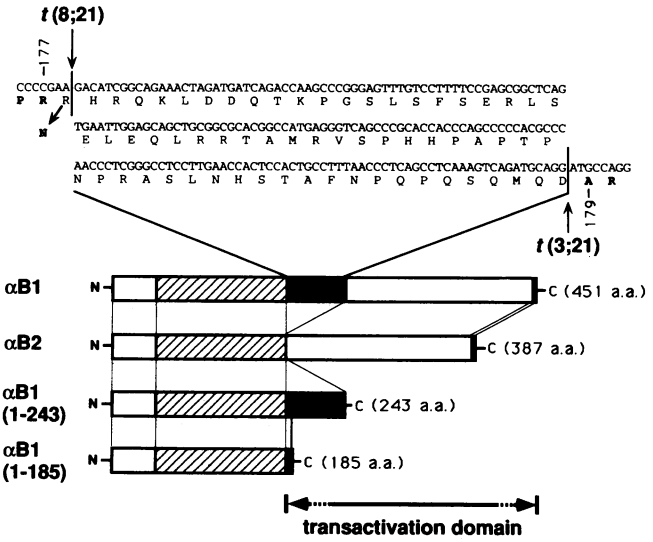

FIG. 6. Diagrammatic representation of the protein structures of αB1, αB2, and deletion constructs αB1(1–243) and αB1(1–185). Hatched boxes represent the Runt domain. ΔαB2 is marked by gray boxes. αB1(1–243) and αB1(1–185) are nearly identical to the human AML1 proteins described previously by Miyoshi et al. (27) and Nisson et al. (29), respectively. The approximate location of the transactivation domain is indicated.

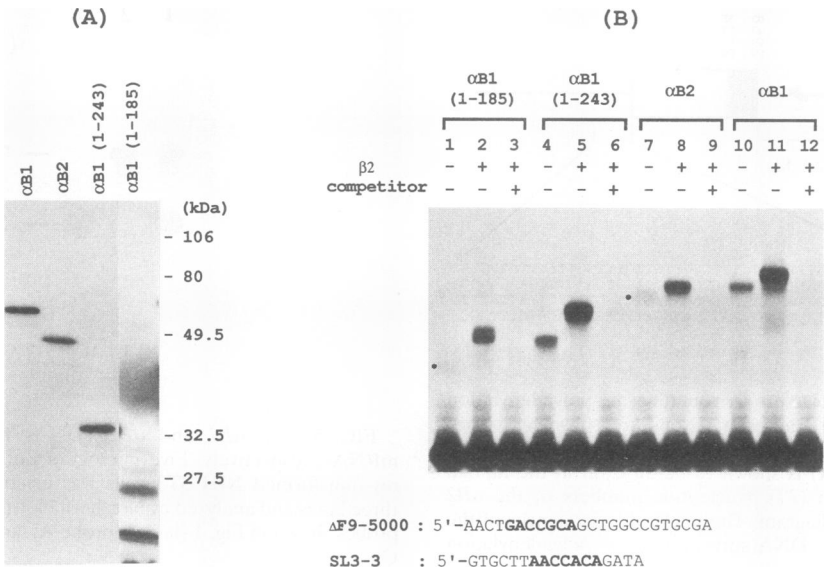

FIG. 7. DNA binding and heterodimerization of in vitro-translated αB1 and αB2 proteins. (A) In vitro translation. The *αB1* and *αB2* cDNAs and their derivative cDNAs in Bluescript II KS$^-$ (Stratagene) were transcribed by T3 or T7 RNA polymerase, and the RNAs were translated in rabbit reticulocyte lysate in the presence of [^{3}H]leucine. Translation products were analyzed by SDS-PAGE (12% polyacrylamide gel) followed by fluorography. (B) EMSA. Each of the in vitro-translated proteins was mixed with ^{32}P-labeled ΔF9-5000 enhancer fragment in the presence or absence of a specific competitor (SL3-3) or with β2 protein and incubated at 30°C for 30 min. The reaction products were analyzed by electrophoresis on a 5% nondenaturing polyacrylamide gel. The nucleotide sequences of ΔF9-5000 and the competitor (SL3-3) are shown, with the core sequence of the PEBP2 recognition sequence in boldface. The very weak bands of lanes 1 and 7 are marked by dots.

There are three alternatively spliced forms of PEBP2β. Of them, the β1 and β2 proteins bind to αA1 equally well, while β3 does not (32). We tested whether the major species, β2, would bind to the αB proteins. All of the αB polypeptides showed supershifts in EMSA accompanied by an increase of DNA binding ability when β2 was added (Fig. 7B, lanes 2, 5, 8, and 9). Supershifted bands were all competed for efficiently by the homologous competitor (lanes 3, 6, 9, and 12). These results clearly showed that αB1 and αB2, like αA1 (34), function as α subunits of PEBP2 and that their domains responsible for DNA binding and heteromeric association with the β protein reside in the region upstream of the C-terminal border of the Runt domain.

Extremely high sequence homology between the human and mouse αB proteins and a highly conserved exon-intron structure of the *αB* gene make it possible to predict the positions t(8;21) and t(3;21) breakpoints on the αB mouse proteins (Fig. 6). The N- and C-terminal boundaries of ΔαB2 have been shown to be exon-intron junctions in human *AML1* (27) and are most likely to be so in mouse *αB* (Fig. 4). All breakpoints of t(8;21) so far reported fall within the intron located at the 5′ side of ΔαB2 (9, 15, 22, 26, 27, 30, 42, 46), while in three cases reported, the breakpoints of t(3;21) fall within the intron located at the 3′ side of ΔαB2 (31). Therefore, the results shown in Fig. 7 predict that the chimeric proteins generated by t(8;21) and t(3;21), which correspond to αB2 and αB1, respectively, must have abilities to bind to DNA and associate with the β protein.

Quantitative EMSA. To assess the α-β association more precisely, more quantitative experiments were carried out. Equivalent amounts of αB1 and αB2 translated in vitro were subjected to EMSA with increasing amounts of radiolabeled DNA probe. Figure 8 shows that αB1 (lanes 11 to 15) and αB2 (lanes 1 to 5) bind to DNA with nearly equal efficiency in the absence of the β protein. The addition of β2 caused an increase in the affinity of αB1 by about 6-fold and that of αB2 by about 14-fold. Repeated experiments indicated that αB2 has two- to threefold-higher affinity to DNA (lanes 6 to 10) than αB1 (lanes 16 to 20) in the presence of β2. The results suggest that ΔαB2 modulates the DNA binding activity of the αB protein.

PEBP2αB1 and -αB2 proteins are activators of transcription. It has previously been shown that PEBP2αA stimulates transcription from the herpesvirus thymidine kinase promoter through the PEBP2 site in the TCR β enhancer (34). We examined the transactivation potential of αB proteins by a CAT assay using the same promoter/enhancer system together with P19 embryonal carcinoma cells as a host. P19 cells do not detectably express the *αB* mRNA (unpublished observation) and hence are advantageous for ectopic expression of the protein. αB1 stimulated CAT activity nearly as strongly as αA1 in a PEBP2 site-dependent manner (Fig. 9A). At a relatively low dosage of the effector plasmids, an optimum transactivation by up to 40-fold was observed with αB1 as well as αA1 (Fig. 9B). Curiously, transactivation by these proteins sharply declined at higher dosages. On the other hand, αB2 showed less than 20-fold stimulation at maximum in association with a decreased tendency to self-repress. Two C-terminally truncated proteins, αB1(1–243) and αB1(1–185), showed no detectable levels of activity. Since αB1(1–243) is nearly identical to the 250-aa human AML1 protein, we predict that the 250-aa human AML1 protein has no transcription-stimulating activity. It then follows that *PEBP2αB* encodes at least three isoforms of transcriptional regulators with different levels of activation potential. The results in Fig. 9 also reveal that the transcriptional activation domain(s) is present downstream of the Runt domain. Further analysis is under way to define its exact location.

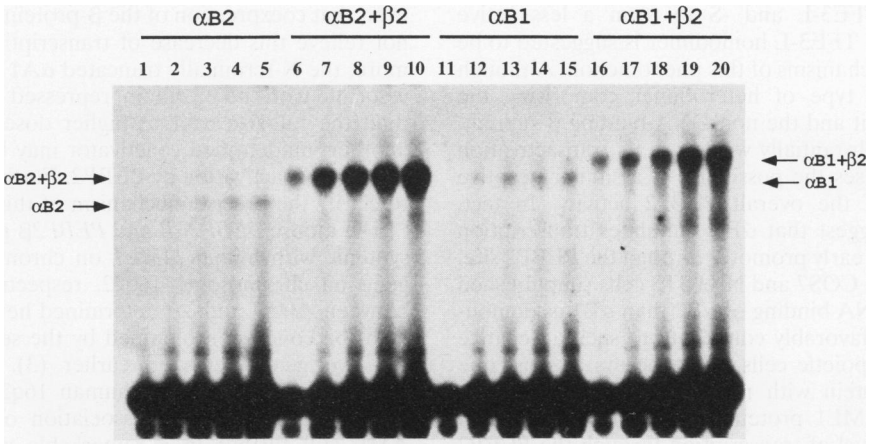

FIG. 8. Comparison of the DNA binding affinities of αB1 and αB2. The in vitro-translated proteins were quantitated by counting the radioactivity of incorporated [^{3}H]leucine of the proteins and SDS-PAGE followed by fluorography and densitometric analysis. Equivalent amounts of αB1 or αB2 (about 0.05 nM for each lane) with or without β2 subunit (0.5 nM for each lane) were incubated with a specified concentration of the probe DNA and subjected to EMSA (lanes 1, 6, 11, and 16, 0.1 nM; lanes 2, 7, 12, and 17, 0.2 nM; lanes 3, 8, 13, and 18, 0.3 nM; lanes 4, 9, 14, and 19, 0.4 nM; lanes 5, 10, 15, and 20, 0.5 nM).

DISCUSSION

Mouse fibroblasts express only two major *PEBP2αB* transcripts, 7.9- and 3.8-kb species, which appear to be a subset of transcripts expressed in hematopoietic cells. A remarkable finding is that the 3.8- and 7.9-kb transcripts specifically encode two distinct proteins, αB1 and αB2, respectively. Peculiarly, αB2 binds to DNA two to three times more strongly than αB1 but is only 25 to 45% as active as the latter in transcription activation. In the 7.9-kb RNA, a 192-base-long region coding for an internal 64-aa sequence is spliced out. This transcript instead contains much longer 5′ and 3′ noncoding regions than does the 3.8-kb RNA. The 3′-terminal length heterogeneity was shown to be due to the alternative choice of polyadenylation sites. On the other hand, the differing 5′-terminal extensions were presumed to involve either alternative RNA splicing or promoter utilization or both. Further structural and functional analyses are required to clarify the mechanism and significance of such differential splicing, polyadenylation, and transcription initiation.

There are a number of cases known in which an alternatively spliced isoform of a transcription factor having a reduced ability of transactivation is synthesized from a single gene in addition to a fully active one. They include FosB, CREM, and mTFE3 (reviewed in reference 10). In the case of mTFE3, one of the isoforms, mTFE3-S, is 30% as active as the other one, mTFE3-L. Small changes in substoichiometric amounts of mTFE3-S result in transdominant negative regulation of mTFE3 activity (38). The heterodimerization of a helix-loop-

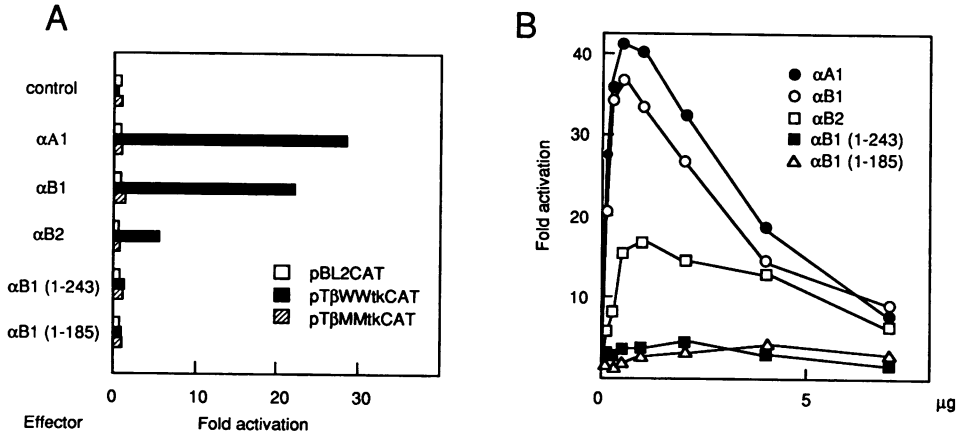

FIG. 9. Multiple forms of transcriptional regulators encoded by αB. (A) Levels of activation of transcription induced by αB1, αB2, and their derivatives. P19 cells, lacking endogenous PEBP2, were cotransfected with 2 μg of reporter plasmid pBL2CAT, pTβ3W4W-tkCAT (pTβWWtkCAT), or pTβ3M4M-tkCAT (pTβMMtkCAT), together with 1 μg each of effector plasmids EF-αA1, EF-αB1, EF-αB2, EF-αB1(1–243), and EF-αB1(1–185). The backbone plasmid, pEF-BOS, alone was tested in parallel as a control. CAT activities were assayed as described in Materials and Methods. The results are displayed as relative ratios of percent acetylation to the control in which pBL2CAT was used as a reporter with pEF-BOS alone. The values are averages of three independent experiments. (B) Dose dependency of transcription activation. Transfection and CAT assays were carried out as in panel A, using 2 μg of pTβ3W4W-tkCAT as a reporter plasmid with indicated amounts of effector plasmids. Results are displayed as relative ratios of percent acetylation to the control without effector. Two independent experiments were carried out with essentially the same results. A typical result is displayed.

helix containing in TFE3-L and -S to form a less active transactivator than the TFE3-L homodimer is suggested to be one of the possible mechanisms of this phenomenon. Although PEBP2 is a different type of heterodimer comprising the DNA-binding α subunit and the non-DNA-binding β subunit, the fact that αB2 is substantially weaker in its transactivation potential than αB1 raises the possibility of a similar negative regulation by αB2 of the overall PEBP2 activity. In fact, preliminary results suggest that αB1 stimulates transcription from the polyomavirus early promoter through the PEBP2 site, while αB2 inhibits it in COS7 and NIH 3T3 cells (unpublished data). The stronger DNA binding of αB2 than αB1 as demonstrated in vitro could favorably contribute to such a negative regulation. In hematopoietic cells, there occurs at least one more type of αB protein with no transactivation function, namely, the 250-aa AML1 protein. This protein also could negatively affect the level of transcription through the PEBP2 site in a similar and supposedly more exaggerated fashion. It appears, therefore, that various degrees of transcription activation through the PEBP2 site could be achieved by changing the relative amounts of multiple isoforms of the αB protein.

Identification of αB2 protein provided valuable information on the boundary of the DNA binding and dimerization domain of the α subunit. We reported earlier that the C-terminal boundary of the Runt domain is the exon-intron junction within which the t(8;21) breakpoints are clustered, since a very high amino acid sequence homology between the α proteins and Runt protein coincidentally ends there (12). The Runt domain defined by this boundary, which also coincides with the N-terminal boundary of ΔαB2, however, nearly completely excludes a cluster of basic amino acids, RRHRQK, which has been suggested to be involved in the DNA binding of the protein (8, 9). We reported earlier that a fragment of the αA1 protein containing mainly the Runt domain having five more amino acids (RHRQK) extending toward the C-terminal direction binds to DNA and dimerizes with the β protein (34). The results presented in this report clearly showed that neither the RHRQK basic stretch nor an arginine residue at the C-terminal end of the Runt domain defined above is required for either activity.

The 64-aa-long segment, ΔαB2, is interesting in several respects. The N- and C-terminal boundaries of ΔαB2 coincide with the positions of the introns within which the breakpoints of t(8;21) and t(3;21), respectively, are clustered. We found that at least one of the important functions of ΔαB2 is to modulate the DNA binding affinity of the αB protein. ΔαB2 is located immediately adjacent to the Runt domain. Thus, the presence or absence of ΔαB2 would more or less directly affect the conformational state of the Runt domain to be involved in DNA binding. Since the β protein acts to strengthen the affinity of the αB protein for DNA, it is equally possible that ΔαB2 indirectly affects DNA binding by modulating the protein-protein interaction between the αB and β proteins. Interestingly, there is also a similar small exon at exactly the same position of the αA1 protein which is highly homologous to ΔαB2 (21). Curiously, the BLAST search (1) revealed a 30-aa region within ΔαB2 which is 66% homologous to a region of the *Drosophila engrailed* protein located adjacent to the homeodomain. This region of the *engrailed* protein is also encoded in a small exon (36). It would be interesting to determine whether these two regions have similar functions.

As for the decrease of transactivation at higher doses of the α proteins, one possible underlying mechanism would be an imbalance of the relative ratio between the α and β subunits. It is conceivable that the β protein is titrated out by higher amounts of the α protein. Preliminary results indicated, however, that coexpression of the β-protein expression plasmid did not relieve this decrease of transcription activation. Furthermore, the N-terminally truncated αA1 protein, which can still associate with the β protein, repressed transcription much less than the full-size αA1 at higher doses (33). Therefore, still another, unidentified coactivator may be involved in the process of transactivation by PEBP2. Further studies are required to clarify the precise mechanism of this phenomenon.

The mouse *PEBP2αB* and *PEBP2β* genes were found to be syntenic with human *AML1* on chromosome 21q22 and the gene on chromosome 16q22, respectively. The relationship between *AML1* and *αB* determined here is entirely consistent with the conclusion obtained by the sequence comparison of the two genes reported earlier (3). The identification of *PEBP2β* as syntenic with human 16q22, on the other hand, reinforced the intimate association of PEBP2 with human AML still further in a remarkable way. Inversion 16 is a frequently observed chromosome abnormality in AML and classified into the FAB-M4Eo subtypes (39). The gene on chromosome 16q22 which is fused to the gene on 16p13 as a result of inversion 16 was indeed found to be the human homolog of PEBP2β (17). Therefore, from our results obtained by using a mouse transcription factor, we could deduce the properties of the human counterpart. We showed that the products of these two mouse genes, *PEBP2αB*/mouse *AML1* and *PEBP2β*/*CBFβ*, form a heterodimer and function as a PEBP2 site-dependent transcription factor. This is the first example in which the genes encoding both subunits of a heterodimeric transcription factor are found at the translocation breakpoints in human leukemia. This, in turn, strongly suggests that both subunits of PEBP2 have indispensable functions in vivo, acting together as an important transcriptional regulator for the growth and differentiation of cells of myeloid lineage and that abnormalities of PEBP2 may account for the pathogenesis of 17 to 20% of AML.

The results presented in this report further provided important insight into how the chimeric proteins AML1/MTG8 (ETO) and AML1-EAP might function. The Runt domain is always included in both types of the chimeras so far examined. We have unequivocally shown in this report that the DNA binding and dimerization activities of αB proteins are harbored in the region upstream of the C-terminal boundary of the Runt domain. It has recently been shown that AML1/MTG8(ETO) indeed binds to the PEBP2 consensus sequence (24). Our results indicate that both types of chimeric proteins retain the potential not only to bind to the PEBP2 site but also to dimerize with the β subunit.

The most crucial activity in the C-terminal region of the αB protein would be its transactivation function. As discussed above, the differential splicing appears to constitute an important regulatory mechanism of gene expression by *AML1*/*αB*. The chimeric proteins completely lose transactivation activity due to AML1 in association with the potency to generate different isoforms of variable functions as suggested for AML1/αB. AML1/MTG8(ETO) may act as a positive transactivator or a negatively interfering factor, depending entirely on whether the MTG8(ETO) moiety has a transactivation function. In either case, such an ectopic transcriptional regulation due to MTG8(ETO) through PEBP2 site would be a possible mechanism of leukemogenesis caused by the t(8;21) translocation. On the other hand, AML1-EAP is most likely devoid of transactivation activity, since an out-of-frame fusion takes place, resulting in the fusion of 17 out-of-frame residues to the C-terminal of the truncated AML1. Direct comparison of two abnormal proteins generated by two different types of translocation at the *AML1* locus will be important to understand the

precise mechanism of leukemogenesis caused by these translocations.

ACKNOWLEDGMENTS

We thank B. Cho for excellent technical assistance.

This research was supported in part by Grants-in-Aid for Special Project Research on Cancer Bio-Science for Cancer Research to (Y.I.) and by the National Cancer Institute under contract NO1-CO-74101 with ABL for (N.A.J. and N.G.C.).

REFERENCES

1. **Altschul, S. F., W. Gish, W. Miller, E. W. Myers, and D. J. Lipman.** 1990. Basic local alignment search tool. J. Mol. Biol. **215:**403–410.
2. **Asano, M., Y. Murakami, K. Furukawa, Y. Yamaguchi-Iwai, M. Satake, and Y. Ito.** 1990. A polyomavirus enhancer binding protein, PEBP5, responsive to 12-*O*-tetradecanoylphorbol-13-acetate but distinct from AP1. J. Virol. **64:**5927–5938.
3. **Bae, S. C., Y. Yamaguchi-Iwai, E. Ogawa, M. Maruyama, M. Inuzuka, H. Kagoshima, K. Shigesada, M. Satake, and Y. Ito.** 1993. Isolation of *PEBP2αB* cDNA representing the mouse homolog of human acute myeloid leukemia gene, *AML1*. Oncogene **8:**809–814.
4. **Boral, A. L., A. Okenquist, and J. Lenz.** 1989. Identification of the SL3-3 virus enhancer core as a T-lymphoma cell-specific element. J. Virol. **63:**76–84.
5. **Chen, C., and H. Okayama.** 1987. High-efficiency transformation of mammalian cells by plasmid DNA. Mol. Cell. Biol. **7:**2745–2752.
6. **Chomczynski, P., and N. Sacchi.** 1987. Single-step method of RNA isolation by acid guanidinium thiocyanate-phenol-chloroform extraction. Anal. Biochem. **162:**156–159.
7. **Copeland, N. G., and N. A. Jenkins.** 1991. Development and applications of a molecular genetic linkage map of the mouse genome. Trends Genet. **7:**113–118.
8. **Daga, A., J. E. Tighe, and F. Calabi.** 1992. Leukemia/*Drosophila* homology. Nature (London) **356:**484.
9. **Erickson, P., J. Gao, K.-S. Chang, T. Look, E. Whisenant, S. Raimondi, R. Lasher, J. Trujillo, J. Rowley, and H. Drabkin.** 1992. Identification of breakpoints in *t*(8;21) acute myelogenous leukemia and isolation of a fusion transcript, *AML1/ETO* with similarity to *Drosophila* segmentation gene *runt*. Blood **80:**1825–1831.
10. **Foulkes, N. S., and P. Sassone-Corsi.** 1992. More is better: activators and repressors from the same gene. Cell **68:**411–414.
11. **Jiang, W., P. M. Sadler, N. A. Jenkins, D. J. Gilbert, N. G. Copeland, and J. S. Bond.** 1993. Tissue-specific expression and chromosomal localization of the α subunit of mouse meprin A. J. Biol. Chem. **268:**10380–10385.
12. **Kagoshima, H., K. Shigesada, M. Satake, Y. Ito, N. Miyoshi, M. Ohki, M. Pepling, and P. Gergen.** 1993. The Runt-domain; identifies a new family of heteromeric transcriptional regulators. Trends Genet. **9:**338–341.
13. **Kamachi, Y., E. Ogawa, M. Asano, S. Ishida, Y. Murakami, M. Satake, Y. Ito, and K. Shigesada.** 1990. Purification of a mouse nuclear factor that binds to both the A and B cores of the polyomavirus enhancer. J. Virol. **64:**4808–4819.
14. **Kania, M. A., A. S. Bonner, J. B. Duffy, and J. P. Gergen.** 1990. The *Drosophila* segmentation gene *runt* encodes a novel nuclear regulatory protein that is also expressed in the developing nervous system. Genes Dev. **4:**1701–1713.
15. **Kozu, Y., H. Miyoshi, K. Shimizu, N. Maseki, Y. Kaneko, H. Asou, N. Kamada, and M. Ohki.** 1993. Junctions of the *AML1/MTG8(ETO)* fusion are constant in t(8;21) acute myeloid leukemia detected by reverse transcription polymerase chain reaction. Blood **82:**1270–1276.
16. **Krimpenfort, P., R. de Jong, Y. Uematsu, Z. Demic, S. Ryser, H. von Boehmer, M. Steinmetz, and A. Berns.** 1988. Transcription of T cell receptor β-chain genes is controlled by a downstream regulatory element. EMBO J. **7:**745–750.
17. **Liu, P., S. A. Tarle, A. Hajra, D. F. Claxton, P. Marlton, M. Freedman, M. J. Siciliano, and F. S. Collins.** 1993. Fusion between transcription factor CBFβ/PEBP2β and a myosin heavy chain in acute myeloid leukemia. Science **261:**1041–1044.
18. **Luckow, B., and G. Schütz.** 1987. CAT constructions with multiple unique restriction sites for the functional analysis of eukaryotic promoters and regulatory elements. Nucleic Acids Res. **15:**5490.
19. **Maniatis, T., E. F. Fritsch, and J. Sambrook.** 1982. Molecular cloning: a laboratory manual. Cold Spring Harbor Laboratory, Cold Spring Harbor, N.Y.
20. **Martin, M. E., X. Y. Yang, and W. R. Fork.** 1992. Expression of a 91-kilodalton PEA3-binding protein is down-regulated during differentiation of F9 embryonal calcinoma cells. Mol. Cell. Biol. **12:**2213–2221.
21. **Maruyama, M., and Y. Ito.** Unpublished data.
22. **Maseki, N., Y. Miyoshi, K. Shimizu, C. Homma, M. Ohki, M. Sakurai, and Y. Kaneko.** 1993. The 8;21 translocation in acute myeloid leukemia is always detectable by molecular analysis using *AML1*. Blood **81:**1573–1579.
23. **Meijer, D., A. Hermans, M. von Lindern, T. van Agthoven, A. de Klein, P. Mackenbach, A. Grootegoed, D. Talarico, G. D. Valle, and G. Grosveld.** 1987. Molecular characterization of the testis specific c-abl mRNA in mouse. EMBO J. **6:**4041–4048.
24. **Meyers, S., J. R. Downing, and S. W. Hiebert.** 1993. Identification of AML1 and the (8;21) translocation protein (AML-1/ETO) as sequence-specific DNA-inding proteins: the runt homology domain is required for DNA binding and protein-protein interactions. Mol. Cell. Biol. **13:**6336–6345.
25. **Michael, A. I., H. F. David, J. S. John, J. W. Thomas.** 1990. PCR protocol: A guide to methods and applications. Academic press, San Diego.
26. **Miyoshi, H., T. Kozu, K. Shimizu, K. Enomoto, N. Maseki, Y. Kaneko, N. Kamada, and M. Ohki.** 1993. The t(8;21) translocation in acute myeloid leukemia results in production of an AML1-MTG8(ETO) fusion transcript. EMBO J. **12:**2715–2721.
27. **Miyoshi, H., K. Shimizu, K. J. Tomoko, N. Maseki, Y. Kaneko, and M. Ohki.** 1991. t(8;21) breakpoints on chromosome 21 in acute myeloid leukemia are clustered within a limited region of a single gene, AML1. Proc. Natl. Acad. Sci. USA **88:**10431–10434.
28. **Mizushima, S. and S. Nagata.** 1990. pEF-BOS, a powerful mammalian expression vector. Nucleic acid Res. **18:**5322.
29. **Nisson, P. E., P. C. Watkins, and N. Sacchi.** 1992. Transcriptionally active chimeric gene derived from the fusion of the AML1 gene and a novel gene on chromosome 8 in t(8;21) leukemic cells. Cancer Genet. Cytogenet. **63:**81–88.
30. **Nucifora, G., D. J. Birn, P. Erickson, J. Gao, M. M. LeBeau, H. A. Drabkin, and J. D. Rowley.** 1993. Detection of DNA rearrangements in the AML1 and ETO loci and of an AML1/ETO fusion mRNA in patients with t(8;21) acute myeloid leukemia. Blood **81:**883–888.
31. **Nucifora, G., C. R. Begy, P. Erickson, H. A. Drabkin, and J. D. Rowley.** 1993. The 3;21 translocation in myelodysplasia results in a fusion transcript between the *AML1* gene and the gene for *EAP*, a highly conserved protein associated with the Epstein-Barr virus small RNA EBER1. Proc. Natl. Acad. Sci. USA **90:**7784–7788.
32. **Ogawa, E., M. Inuzuka, M. Maruyama, M. Satake, M. Naito-Fujimoto, Y. Ito, and K. Shigesada.** 1993. Molecular cloning and characterization of PEBP2β, the heterodimeric partner of a novel *Drosophila runt*-related DNA binding protein PEBP2α. Virology **194:**314–331.
33. **Ogawa, E., and Y. Ito.** Unpublished data.
34. **Ogawa, E., M. Maruyama, H. Kagoshima, M. Inuzuka, J. Lu, M. Satake, K. Shigesada, and Y. Ito.** 1993. PEBP2/PEA2 represents a new family of transcription factor homologous to the products of the *Drosophila runt* and the human *AML1*. Proc. Natl. Acad. Sci. USA **90:**6859–6863.
35. **Piette, J., and M. Yaniv.** 1987. Two different factors bind to the α-domain of the polyoma virus enhancer, one of which also interacts with the SV40 and *c-fos* enhancers. EMBO J. **6:**1331–1337.
36. **Poole, S. J., L. M. Kauvar, B. Drees, and T. Kornberg.** 1985. The *engrailed* locus of *Drosophila*: structural analysis of an embryonic transcript. Cell **40:**37–43.
37. **Redondo, J. M., J. L. Pfohl, C. Hernandez-Munain, S. Wang, N. A. Speck, and M. S. Krangel.** 1992. Indistinguishable nuclear factor binding to functional core sites of the T-cell receptor δ and murine leukemia virus enhancers. Mol. Cell. Biol. **12:**4817–4823.

38. **Roman, C., L. Cohon, and K. Calame.** 1991. A dominant negative form of transcription activator mTFE3 created by differential splicing. Science **254:**94–97.
39. **Rowley, J. D.** 1984. Biological implications of consistent chromosome rearrangements in leukemia and lymphoma. Cancer Res. **44:**3159–3168.
40. **Sakakura, C., Y. Yamaguchi-Iwai, M. Satake, S. C. Bae, A. Takahashi, A. Hagiwara, T. Takahashi, N. Kamada, and Y. Ito.** Growth inhibition and induction of differentiation of *t*(8;21) acute myeloid leukemia cells by the DNA binding domain of PEPB2 and the *AML1/MTG8(ETO)* specific antisense oligonucleotide. Submitted for publication.
41. **Sambrook, J., E. F. Fritsch, and T. Maniatis.** 1988. Molecular cloning: a laboratory manual, 2nd ed. Cold Spring Harbor Laboratory, Cold Spring Harbor, N.Y.
42. **Shimizu, K., H. Miyoshi, T. Kozu, J. Nagata, K. Enomoto, N. Maseki, Y. Kaneko, and M. Ohki.** 1992. Consistent disruption of the *AML1* gene occurs within a single intron in the t(8;21) chromosomal translocation. Cancer Res. **52:**6945–6948.
43. **Siracusa, L. D., N. A. Jenkins, and N. G. Copeland.** 1991. Identification and applications of repetitive probes for gene mapping in the mouse. Genetics **127:**169–180.
44. **Suzou, J., and A. D. Friedman.** 1993. The murine myeloperoxidase promoter contain several functional elements, one of which bind a cell type-restricted transcription factor, myeloid nuclear factor I (MyNF1). Mol. Cell. Biol. **13:**2141–2151.
45. **Thornell, A., B. Hallberg, and T. Grundstrom.** 1988. Differential protein binding in lymphocytes to a sequence in the enhancer of the mouse retrovirus SL3-3. Mol. Cell. Biol. **8:**1625–1637.
46. **Tighe, J. E., A. Daga, and F. Calabi.** 1993. Translocation breakpoints are clustered on both chromosome 8 and chromosome 21 in the t(8;21) of acute myeloid leukemia. Blood **81:**592–596.
47. **Wang, S., and N. A. Speck.** 1993. Purification of core-binding factor, a protein that binds the conserved core site in murine leukemia virus enhancers. Mol. Cell. Biol. **12:**89–102.
48. **Xin, J.-H., A. Cowie, P. Lachance, and J. A. Hassell.** 1992. Molecular cloning and characterization of PEA3, a new member of the *Ets* oncogene family that is differentially expressed in mouse embryonic cells. Genes Dev. **6:**481–496.
49. **Xiong, Y., T. Connolly, B. Futcher, and D. Beach.** 1991. Human D type cyclin. Cell **65:**691–699.